

# Application of Feed Forward Neural Networks for modeling of heat transfer coefficient during flow condensation for low and high values of saturation temperature

**Stanisław Głuch<sup>a</sup>, Tacjana Niksa-Rynkiewicz<sup>b</sup>, Dariusz Mikielawicz<sup>c</sup> and Piotr Stomma<sup>d</sup>**

<sup>a</sup> Gdańsk University of Technology, Gdańsk, Poland [stanislaw.gluch@pg.edu.pl](mailto:stanislaw.gluch@pg.edu.pl)

<sup>b</sup> Gdańsk University of Technology Gdańsk, Poland [tacjana.niksa@pg.edu.pl](mailto:tacjana.niksa@pg.edu.pl)

<sup>c</sup> Gdańsk University of Technology Gdańsk, Poland [dariusz.mikielawicz@pg.edu.pl](mailto:dariusz.mikielawicz@pg.edu.pl)

<sup>d</sup> University of Białystok, Białystok, Poland, [p.stomma@uwb.edu.pl](mailto:p.stomma@uwb.edu.pl)

## Abstract:

Most of the literature models for condensation heat transfer prediction are based on specific experimental parameters and are not general in nature for applications to fluids and non-experimental thermodynamic conditions. Nearly all correlations are created to predict data in normal HVAC conditions below 40 °C. High temperature heat pumps operate at much higher parameters. This paper aims to create a general model for the calculation of heat transfer coefficients during flow condensation which could be applied to a wide range of fluids and thermodynamical parameters up to the vicinity of the critical point. To achieve this goal authors present a model based on Feed Forward Neural Network. The designed neural network consists of 5 hidden layers and utilizes ReLu and linear activation functions. The first four layers consist of 50 neurons, and the last layer consists of 1 neuron. The network was trained on a consolidated database which consists of 4659 data points for 25 fluids and covers a range of reduced pressure from 0.1 to 0.9 for various mass velocities and diameters. Two input variants were considered. For randomly selected test data Mean Square Root achieved 0.1093 and Mean Absolute Error MAE achieved 0.2243 for the first configuration which consist of 4 parameters. For the second variant, which consists of 17 parameters, MSE achieved 0.0452 MAE achieved 0.1028.

## Keywords:

condensation; heat transfer coefficient; high value of reduced pressure; increased saturation pressure; artificial neural network.

## 1. Introduction

The condensation process in high temperature heat pumps occurs at temperatures higher than 80 °C. There is a knowledge gap in the literature for increased saturation temperatures above 90 °C. There is sparse data for the corresponding high reduced pressures for lower values of saturation temperature. Most of existing experimental data is collected for temperatures below 40 °C, which is related to the refrigeration applications of low boiling agents. For temperatures higher than 120 °C most refrigerants operate around the thermodynamic critical point, where rapid changes in viscosity and density of the liquid and vapor phases occur, which has a significant impact on interfacial interactions. During the 2022 energy price crisis increased demand could be observed for industrial high temperature heat pumps (HTHP). These devices enable energy recovery and further utilization in industrial processes. High temperature heat pumps operate in the vicinity of the critical point. Among the others, the thermal and hydraulic issues close to the critical point are the least recognized. The larger amount of works are related only to carbon dioxide, much smaller to water. Studies for other fluids are very scarce. The ones published are presented in a consolidated database. Only a few experiments regard condensation at high saturation temperatures in the near critical area. The basic characteristics in flows through the channels at close to critical parameters have been studied since the 50s of last century. Nevertheless, the phenomena presenting the specific challenges for the successive researchers have been observed and can be outlined as follows: 1) The fluid is very expandable, while the thermal diffusivity tends to zero due to very low thermal conductivity and high specific heat. 2) The thermal properties change nonlinearly, which is different from the normal liquid or gas flow and leads to new flow structures. 3) The absence of surface tension and a capillary effect leads to low pressure loss and low flow friction. 4) The buoyancy effect can be more complex. 5) There are expected thermal-mechanical effects and

several time and spatial scales, related to thermal equilibrium or stability evolution in confined spaces. Recently, because of environmental protection requirements, it's an obligation to look for new working fluids, in the case in which physical characteristics are not sufficiently studied. In addition, a large group of these fluids are mixtures. In such a case, the issue is further complicated. It's hard to define the close to the critical area due to the temperature glide effect as well as the different thermal and flow properties of the mixture components. As a result, there is a risk of the formation of vapor-liquid mixtures with dynamics difficult to control. This may happen when one (or more) of the mixture components passes the critical point, while the other components remain in the subcritical area. The situation is similar for media containing additives, i.e. refrigerant oils, air, or inert gases. Untypical character and high dynamics of phenomena taking place in the area close to critical require the selection of working parameters of installation to be chosen very carefully. The authors aim to create a general model which can accurately predict the heat transfer coefficient during condensation at various values of reduced pressure. A special focus on parameters in the vicinity of critical point is a novelty of this research. The authors utilized Feed forward Neural Network which has a different structure than the neural network presented by other authors. The new FNN is also significantly smaller.

Work carried out by other researchers is described in paragraph 1. The consolidated database is described in the second paragraph. Feed-forward network model is presented in the next paragraph. The results are discussed in the fourth paragraph.

### 1.1. Prediction methods that utilize neural networks.

The study presented by [1] uses machine learning (ML) methods to predict heat transfer coefficients (HTCs) for flow condensation in horizontal tubes. A database with a wide range of fluids and experimental conditions is compiled to evaluate five ML models. Using XGBoost models, a new universal correlation is developed based on the analysis of the most important parameters. The study finds that the ML models perform well in predicting the 1213 test data points, with convolutional neural network CNN achieving the best mean absolute relative deviation (MARD) of 5.82% and the coefficient of determination ( $R^2$ ) of 0.98 or higher for both XGBoost models. XGBoost is better at extrapolating data with reliable performance and the lowest MARD of 19.64%. They also created a conventional correlation which mean absolute relative difference achieved 19.21%. Qiou et al. [2] gathered a consolidated database of 16953 data points. The consolidated database was divided into training and testing data, and an optimization is performed to create the final model architecture consisting of dimensionless input parameters and hidden layers. The artificial neural network (ANN) model demonstrates excellent accuracy in predicting the test data with a mean absolute error (MAE) of 14.3%, and 92.0%, and 97.4% of the predicted data fall within  $\pm 30\%$  and  $\pm 50\%$ , respectively. The performance of the ANN model was compared with universal correlations for saturated flow boiling heat transfer which was outperformed by ANN. Zhou et al. [3] proposed a new method for predicting heat transfer coefficients in flow condensation in mini/microchannels using a consolidated database of 4,882 data points from 37 sources. The data includes various parameters such as working fluid, reduced pressures, hydraulic diameters, and mass velocities. Four machine learning models were developed and compared, and the ANN and XGBoost models showed the best predicting accuracy. These models were able to predict test data with MAEs of 6.8% and 9.1%, respectively. The models were also compared to a highly reliable universal correlation and were found to perform better in predicting heat transfer coefficients for individual datasheets and different condensation flow regimes. The models were able to accurately predict heat transfer coefficients for datasets outside their training database when fluid specific information was available. The study shows that machine learning algorithms can be used to develop a robust new tool for predicting heat transfer coefficients in flow condensation in mini/micro channels. Moradkhani et al. [4] presented a study which focused on the creation of accurate models for estimating the condensation heat transfer coefficient (HTC) inside conventional and mini/micro channel heat exchangers using machine learning methods. The study evaluated the performance of three different models: gaussian process regression (GPR), hybrid radial basis function (HRBF), and interpolating-based radial basis function (RBF). The study also presented a new general correlation using the least square fitting method (LSFM). The study evaluated the accuracy of earlier HTC models and found a lack of more accurate models for condensation heat transfer coefficient (HTC) in conventional and mini/micro channels. Among the intelligent method-based models, the GPR model showed the highest accuracy for the testing dataset with an average absolute relative deviation of 4.50%, and it was selected as the most reliable model for predicting the HTC in different channels. The study also developed a new conventional general HTC correlation.

## 2. Consolidated database

The consolidated database is presented in the Table 1. It consists of data presented in 28 publications for 21 fluids. Mass velocity varies from 75 to 1400  $\text{kg}/(\text{m}^2 \cdot \text{s})$ , reduced pressure varies from 0.1 to 0.9 and diameters vary from 0.76 mm to 15 mm. The first 22 sources which consist form almost 2900 data points were used to train neural networks. 6 last sources are intended for ANN testing

**Table 1.** Consolidated Database.

number	Authors	Diameter [mm]	Fluid [-]	Mass Velocity G [kg/(m <sup>2</sup> ·s)]	Reduced Pressure Pr [-]	Number of Points [-]
1	Mcdonald et al. [5,6]	0.76-1.45	R290	150-450	0.254-0.809	260
2	Aroonath [7]	8.1	R134a	300-500	0.251-0.325	54
3	Cavallini et al. [8]	8	R22, R410a, R32, R236ea, R134a, R125	100-800	0.307-0.55	251
4	Cavallini et al. [9]	1.4	R134a, R410a	200-1400	0.251	77
5	Cavallini et al. [10]	0.96	R32, R254fa	100-1200	0.068-0.428	117
6	Keiratch [11]	0.86-3	R404a	200-800	0.382-0.618	522
7	Garimella et al. [12]	0.76-1.52	R410a	200-800	0.805-0.899	214
8	Jiang et al. [13]	9.4	R410a, R404a	200-800	0.8005-0.9	416
9	Fonk and Garimella [14]	1.4	R717	75-150	0.103-0.231	75
10	Andersen [15]	3.05	R410a	400-800	0.8	52
11	Del Co et al. [16]	0.96	R1234yf	200-1000	0.3007	67
12	Del Co et al. [17]	0.762	Propane	100-1000	0.3225	63
13	Longo et al. [18]	4	R290, PROPYLENE, R404a	75-300	0.25-0.322	194
14	Longo et al. [19]	4	R32, R410a	100-800	0.33-0.49	159
15	Longo et al. [20]	4	R134a, R152a, R1234yf, R1234ze(e)	75-600	0.13-0.3	280
16	Ghim and Lee [21]	7.75	R245fa	150-500	0.093	20
17	Patel et al. [22]	1	R134a, R1234yf	202-811	0.256-0.3	77
18	Zhuang et al. [23]	4	Ethane	101-255	0.22-0.522	230
19	Song et al. [24]	4	R14	200-650	0.27-0.79	189
20	Zhuang et al. [25]	4	Methane	99-254	0.43-0.76	286
21	Milkie et al. [26]	7.75	R245fa, n-PENTANE	150-600	0.04-0.17	266
22	Keniar and Garimella [27]	1.55	R245fa, R134a, R1234ze(E)	50-200	0.05-0.32	149
23	Moriera et al. [28]	9.43	R134a, PROPYLENE, R290, R600a	50-250	0.12-0.32	140
24	Huang et al. [29]	0.00418	R410a	200-600	0.49	35
25	Illan-Gomez et al. [30]	1.16	R1234yf	350-945	0.23-0.43	219
26	Del Col et al. [31]	1	Propylen	80-1000	0.35	109
27	Azzolin et al. [32]	3.4	R134a	50-200	0.25	73
28	Berto et al. [33]		R245fa	30-150	0.68	124
		0.76-9.4	25 fluids	75-1400	0.103-0.9	1916

### 3. Neural network model

The previously cited studies [1–4] show that the use of the artificial intelligence method can give better results than conventional correlations for predicting the heat transfer coefficient. During the initial tests, 3 methods were investigated: Feedforward Neural Networks (FNN), Convolutional Neural Networks (CNN), and the k-means clustering algorithm. The results provided by FNN were the most promising and the authors decided to

pursue this approach. Artificial Neural Network ANN showcased high quality results also in [34,35]. A multi-layer neural network was developed to train the prediction of the heat transfer coefficient during flow condensation. The scheme of this network is presented in the Figure 1.

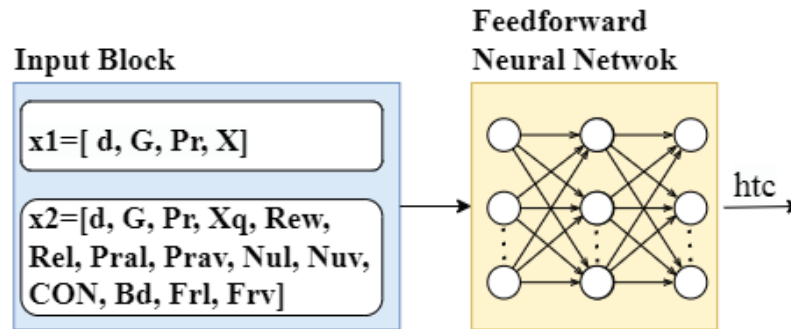


**Figure 1.** Scheme of designed neural network.

The applied neural network uses activation functions (FA), such as ReLu (fR)  $fR(x) = \max(0, x)$  and Linear  $fL(x) = x$ . ReLu is used on 4 first layers, and the last layer utilizes linear function. The authors of the work tried to make the architecture of the network used as simple as possible, and at the same time give the best results. Finally, 5 hidden layers were used with 50 neurons in the first layer (M=50), 50 neurons in the second layer (N=50), 50 neurons in the fourth layer (D=50), 50 neurons in the third layer (P=50), and 1 neuron in the last layer (Q=1). The output ( $y_{out}$ ) signal from the network is described by the relation:

$$y_{out}(x, \omega) = fL\left(\sum_{i=1}^Q \omega_{ji}^I \cdot x_i \left(\sum_{l=1}^P \omega_{out}^l fL\left(\sum_{k=1}^D \omega_{lk}^{II} fR\left(\sum_{j=1}^N \omega_{kj}^I fR\left(\sum_{i=1}^M \omega_{ji}^I \cdot x_i + \omega_{j0}^I\right) + \omega_{k0}^{II}\right) + \omega_{l0}^{IV}\right) + \omega_{l0}^{III}\right)\right) + \omega_{0out0}^{IV} + \omega_{l0}^{III} \quad (1)$$

Signals  $x(k) = [x_1, \dots, x_M]$  given to the input k neuron multiplied by sets of weights  $\omega(k)$  are sent to the next fully connected layer. The vector of initial weights  $\omega(k) = [\omega_1, \dots, \omega_M]$  is randomized from the range (0,1). Given the research results described in [36] the Adam algorithm was used to teach the networks under study. The network performance error was calculated as the difference between expected  $y$  and output  $\hat{y}$  based on Mean Squared Error (MSE) and Mean Average Error (MAE) for all n observations  $i; i = 1.. n$ ;

$$MSE(y, \hat{y}) = 1/n \sum_i^n (y(i) - \hat{y}(i))^2 \quad (1)$$

## 4. Results

FNN was trained for two input data configurations. The first one consisted only of basic thermodynamical parameters: diameter, flow rate, quality, and reduced pressure (in comparison to critical pressure). The second configuration feature also a set of criteria numbers. From the learning database, nearly 800 measurements were randomly selected to test the database. A comparison of the two input configurations is presented in the Table 2. Both configurations achieved good results for the test dataset. Case 1 with only 4 basic input parameters achieved accurate output data of its limited input data. The second configuration achieved significantly better results., which are lower than the measurement errors of most experiments. Most experiments regarding measurement of HTC during condensation have measurement errors between 10 and 20%. It is worth mentioning that the presented ANN was much smaller than the artificial intelligence networks presented by [1–4]. Values of MSE and MAE have achieved thanks to data preparation and curation for FNN. The expected value was turned into a logarithmic value and rescaled, which enabled FNN to achieve formidable results.

**Table 2.** FNN evaluations on the test dataset for different input combinations.

case	number of input parameters	input parameters	MSE	MAE
1	4	d, G, Pr, X	0.1093	0.2243
2	17	d, G, Pr, X, Rev, Rel, Pral, Prav, Nul, Nuv, CON, Bo, Frl, Frv, Frif, Frvf, Wevf	0.0452	0.1028

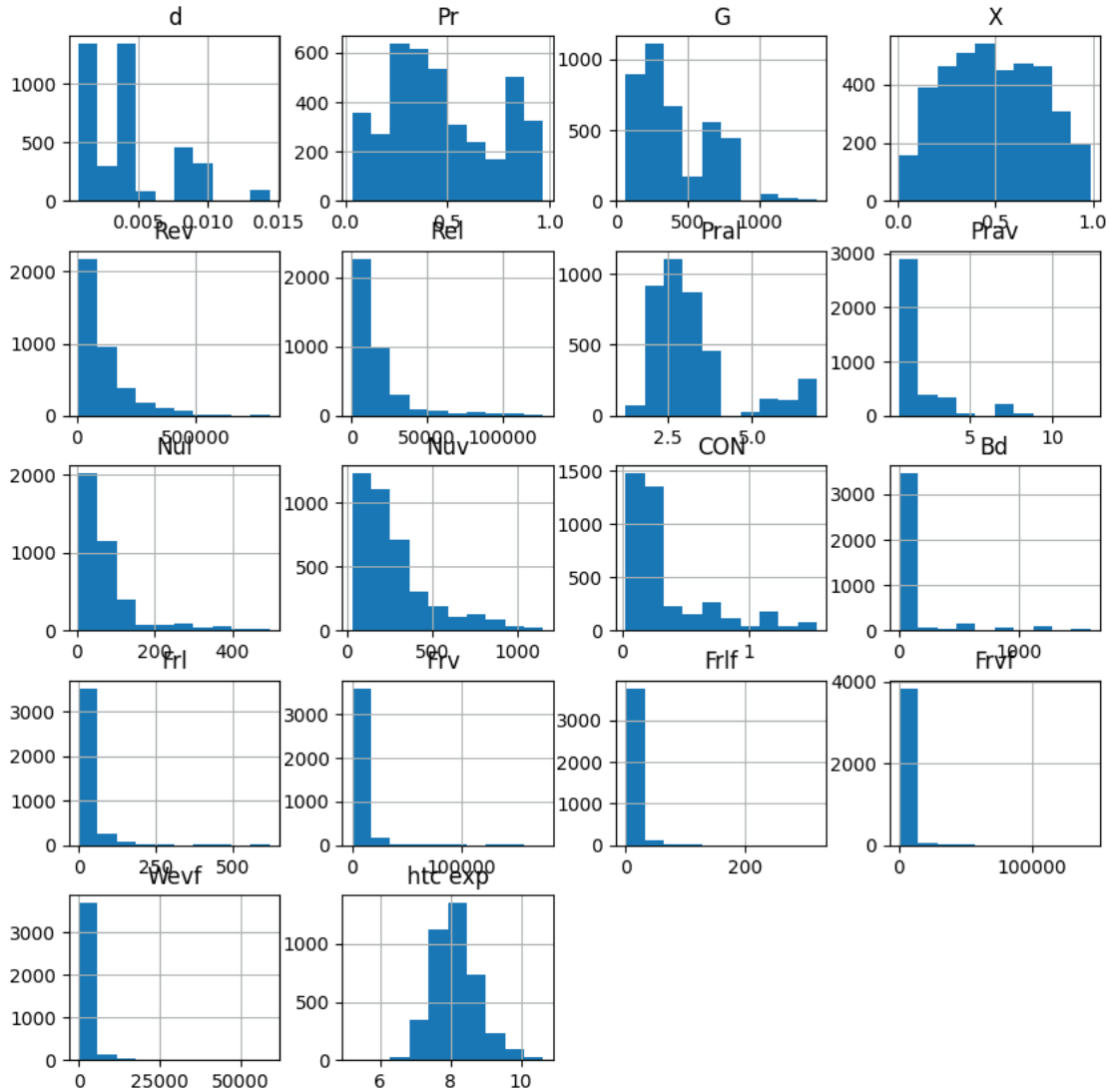


**Figure 2.** Histograms that present the distribution of input parameters.

Histograms which present the distribution of input parameters are present in the Figure 2. Parameters are described in the nomenclature section. Most important are diameter, mass velocity, reduced pressure and quality which are measured during the experiment. The rest of the parameters are criteria numbers which are calculated using fluid properties and mentioned experimental parameters. The learning process of the first dataset can be observed in the Fig. 3. Comparison of experimental and calculated values of HTC can be observed in the Fig. 4 and the Fig. 5. Value of the expected value and output value for the training dataset provides good results for sparse input data. Both variants were trained for 100 epochs.

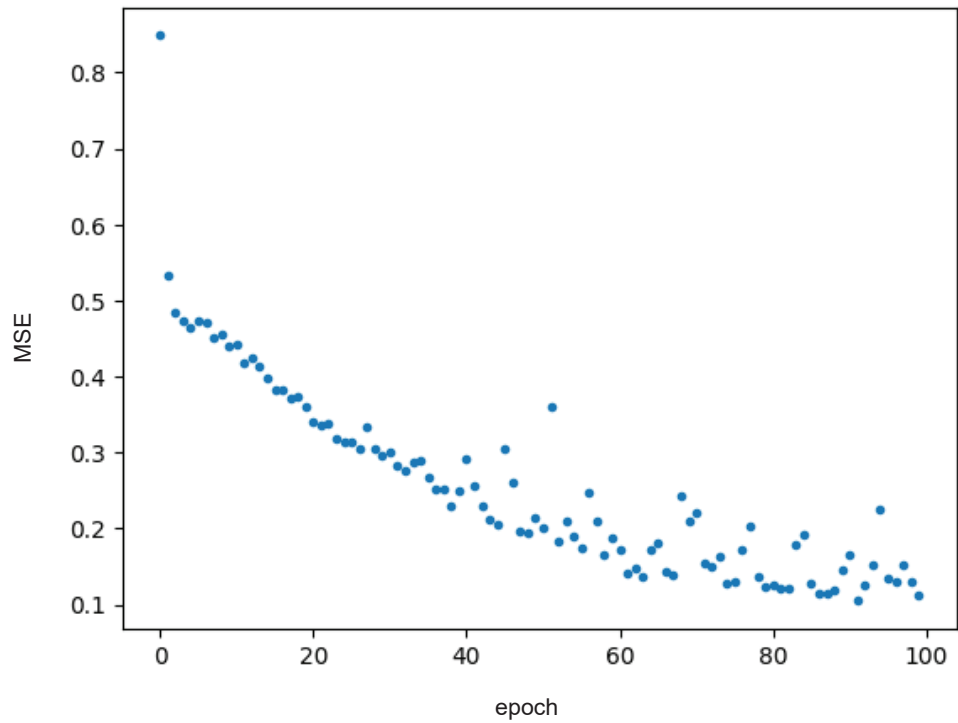


**Figure 3.** Learning graph for the first input configuration

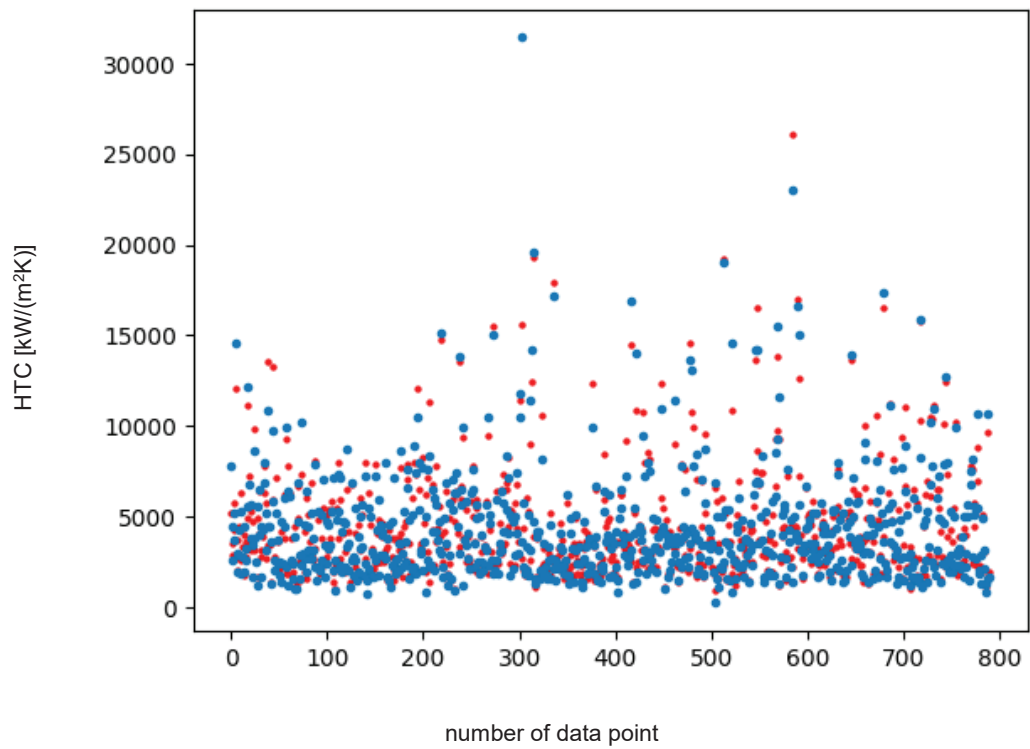


**Figure 4.** Comparison of experimental heat transfer coefficient and results for the first input configuration. Experimental values are blue and FNN output values are red.

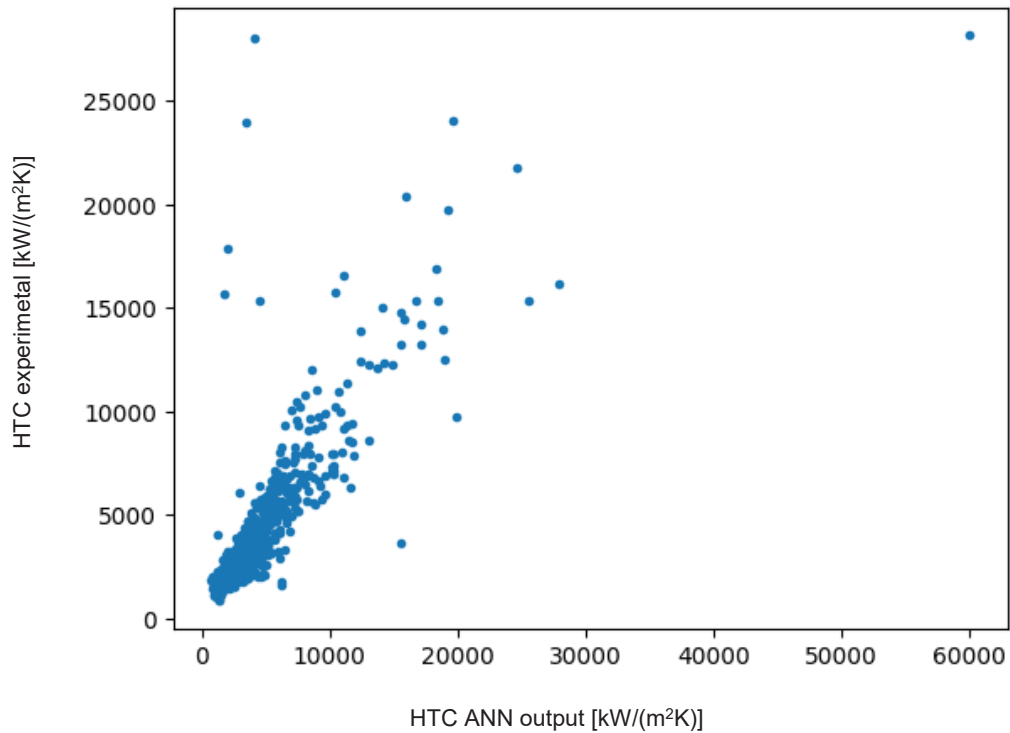


**Figure 5.** Comparison of HTC value measured during the experiment and ANN output data for the first input configuration

The learning process of the second dataset can be observed in the Fig. 6. Comparison of experimental and calculated values of HTC can be observed in the Fig. 7 and in the Fig. 6. Better results can be observed in the Fig. 8. than in the Fig. 4. Learning process is significantly faster f second configuration.

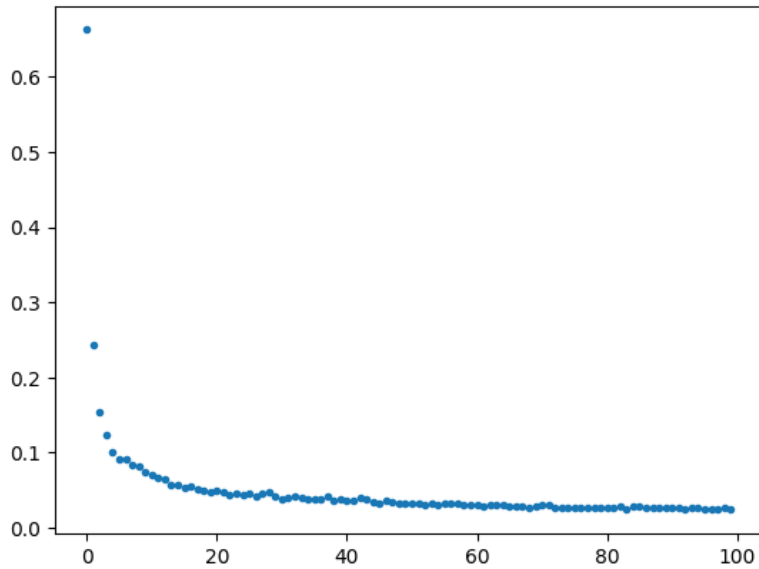


**Figure 6.** Learning graph for the second input configuration

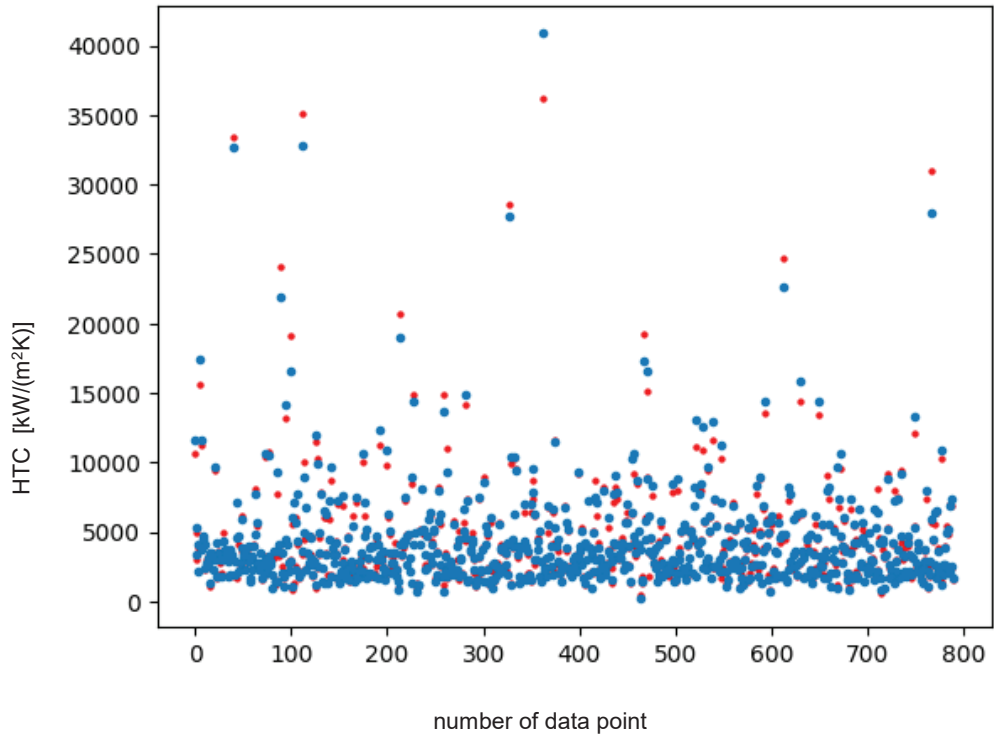


**Figure 7.** Comparison of experimental heat transfer coefficient and results in for the second input configuration. Experimental values are blue and FNN output values are red.

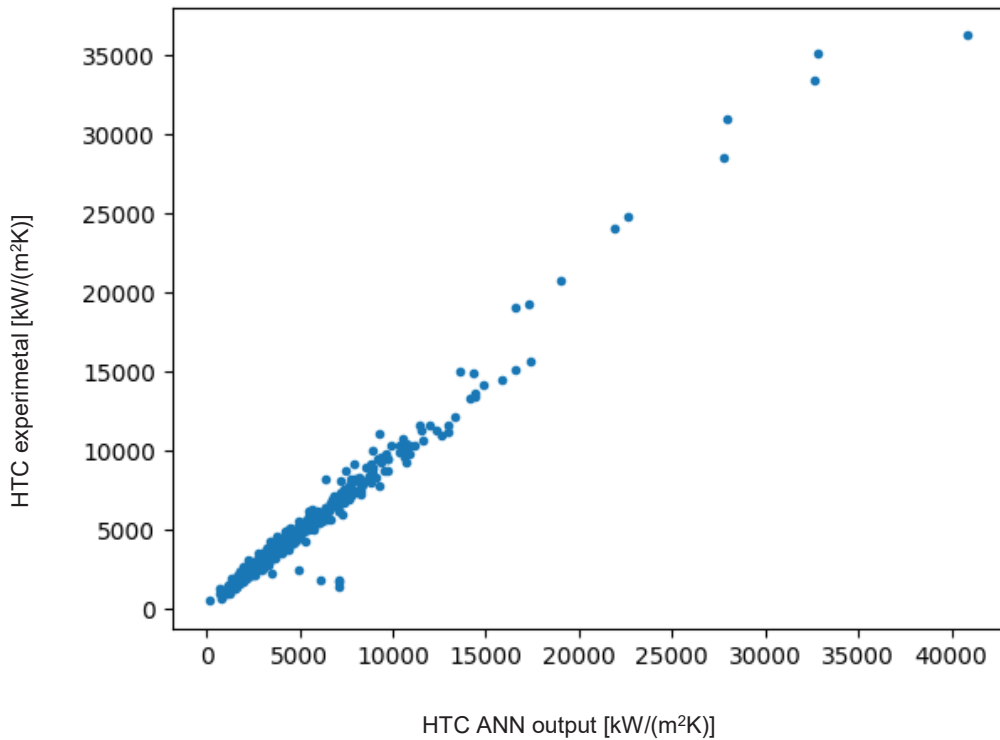


**Figure 8.** Comparison of HTC value measured during the experiment and ANN output data for the second input configuration



## 4. Conclusions

The authors created a model which can predict heat transfer coefficient during flow condensation. The model utilizes Feed Forward Neural Network (FNN). The method was trained on the consolidated experimental database which consists of 4659 data points. The consolidated database covers various parameters of diameter, mass velocities, and reduced pressures ranging from 0.1 to 0.9. The proposed Feed Forward Neural network achieved very good results for randomly selected data points. Designed FNN consists of 5 hidden layers and utilizes ReLu and linear activation functions. ADAM algorithm was used for training. Mean Square Root MSE achieved 0.1093 and Mean Absolute Error MAE achieved 0.2243 for the first variant. For the second variant, MSE achieved 0.0452 MAE achieved 0.1028. The value of MAE achieved by the second configuration is lower than the measurement error of most experiments. It is important to mention that created FNN is relatively small, but it managed to provide good results. The created network consists of 5 layers. Further development of work is required to gather more experimental data points from different experiments than used in testing data and testing created FNN on a new dataset. This will allow to test the new method in a real-case scenario.

## Nomenclature

ANN	Artificial Neural Network,
d	diameter, m
G	mass velocity, $\text{kg}/(\text{m}^2 \cdot \text{s})$
Pr	reduced pressure -ratio of pressure to critical pressure, -
Rel	Reynolds number for saturated liquid $Rel = \frac{GD}{\mu l}$ , -
Rev	Reynolds number for saturated vapour $Rev = \frac{GD}{\mu v}$ , -
t	temperature, °C
Wel	Weber number for saturated liquid $Wel = \frac{G^2 D}{\rho l}$ , -
x	Quality, -
HTC	heat transfer coefficient , $\text{kW}/(\text{m}^2 \text{K})$
FNN	Feed Forward Neural Network, -
ML	Machine Learning, -
CNN	Convolutional Neural Network, -
Pr <sub>l</sub>	Prandtl number for saturated liquid, -
Pr <sub>v</sub>	Prandtl number for saturated vapour, -
Nu <sub>l</sub>	Nusselt number for saturated liquid, -
Nu <sub>v</sub>	Nusselt number for saturated vapour, -
CON	Confinement Number, -
Bo	Bond number, -
Fr <sub>l</sub>	Froude number for saturated liquid, -
Fr <sub>v</sub>	Froude number for saturated vapour, -
Fr <sub>lf</sub>	Froude number for liquid fraction, -
Fr <sub>vf</sub>	Froude number for vapour fraction, -
We <sub>vf</sub>	Weber number for vapour fraction, -

## Acknowledgements

This research was funded in whole or in part by National Science Centre, Poland 2021/41/N/ST8/04421

## References

- [1] Nie F., Wang H., Zhao Y., Song Q., Yan S., Gong M., A Universal Correlation for Flow Condensation Heat Transfer in Horizontal Tubes Based on Machine Learning. International Journal of Thermal Sciences 2023;184:107994.

- [2] Qiu Y., Garg D., Zhou L., Kharangate C.R., Kim S.M., Mudawar I., An Artificial Neural Network Model to Predict Mini/Micro-Channels Saturated Flow Boiling Heat Transfer Coefficient Based on Universal Consolidated Data. *International Journal of Heat and Mass Transfer* 2020;149:.
- [3] Zhou L., Garg D., Qiu Y., Kim S.M., Mudawar I., Kharangate C.R., Machine Learning Algorithms to Predict Flow Condensation Heat Transfer Coefficient in Mini/Micro-Channel Utilizing Universal Data. *International Journal of Heat and Mass Transfer* 2020;162:120351.
- [4] Moradkhani M.A., Hosseini S.H., Song M., Robust and General Predictive Models for Condensation Heat Transfer inside Conventional and Mini/Micro Channel Heat Exchangers. *Applied Thermal Engineering* 2022;201:117737.
- [5] Macdonald M., Garimella S., Hydrocarbon Condensation in Horizontal Smooth Tubes: Part i - Measurements. *International Journal of Heat and Mass Transfer* 2016;93:75–85.
- [6] Macdonald M., Garimella S., Hydrocarbon Condensation in Horizontal Smooth Tubes: Part II - Heat Transfer Coefficient and Pressure Drop Modeling. *International Journal of Heat and Mass Transfer* 2016;93:1248–1261.
- [7] Aroonrat K., Wongwises S., Experimental Study on Two-Phase Condensation Heat Transfer and Pressure Drop of R-134a Flowing in a Dimpled Tube. *International Journal of Heat and Mass Transfer* 2017;106:437–448.
- [8] Cavallini A., Censi G., Col D. Del, Doretti L., Longo G.A., Rossetto L., Experimental Investigation on Condensation Heat Transfer and Pressure Drop of New HFC Refrigerants in a Horizontal Smooth Tube À Rimentale Sur Le Transfert de Chaleur Lors de La Etude Expe Condensation et Sur La Chute de Pression Des Nouveaux Frigorige Da. 2001;24:.
- [9] Cavallini A., Del Col D., Doretti L., Matkovic M., Rossetto L., Zilio C., Condensation Heat Transfer and Pressure Gradient inside Multiport Minichannels. *Heat Transfer Engineering* 2005;26:45–55.
- [10] Cavallini A., Bortolin S., Del Col D., Matkovic M., Rossetto L., Condensation Heat Transfer and Pressure Losses of High- and Low-Pressure Refrigerants Flowing in a Single Circular Minichannel. *Heat Transfer Engineering* 2011;32:90–98.
- [11] Keinath B., Void Fraction, Pressure Drop, and Heat Transfer in High Pressure Condensing Flows through Microchannels. 2012;1–353.
- [12] Garimella S., Andresen U.C., Mitra B., Jiang Y., Fronk B.M., Heat Transfer During Near-Critical-Pressure Condensation of Refrigerant Blends. *Journal of Heat Transfer* 2016;138:.
- [13] Jiang Y., Garimella S., Heat Transfer and Pressure Drop for Condensation of Refrigerant R-404A at Near-Critical Pressures. *ASHRAE Winter Meetings CD, Technical and Symposium Papers* 2003;2003:667–677.
- [14] Fronk B.M., Garimella S., Heat Transfer and Pressure Drop During Condensation of Ammonia in Microchannels 2012;, 399–409.
- [15] Andresen U.C., Supercritical Gas Cooling and Near-Critical-Pressure Condensation of Refrigerant Blends in Microchannels. 2006;
- [16] Del Col D., Torresin D., Cavallini A., Heat Transfer and Pressure Drop during Condensation of the Low GWP Refrigerant R1234yf. *International Journal of Refrigeration* 2010;33:1307–1318.
- [17] Del Col D., Bortolato M., Bortolin S., Comprehensive Experimental Investigation of Two-Phase Heat Transfer and Pressure Drop with Propane in a Minichannel. *International Journal of Refrigeration* 2014;47:66–84.
- [18] Longo G.A., Mancin S., Righetti G., Zilio C., Saturated Vapour Condensation of HFC404A inside a 4 Mm ID Horizontal Smooth Tube: Comparison with the Long-Term Low GWP Substitutes HC290 (Propane) and HC1270 (Propylene). *International Journal of Heat and Mass Transfer* 2017;108:2088–2099.
- [19] Longo G.A., Mancin S., Righetti G., Zilio C., Saturated Vapour Condensation of R410A inside a 4 mm ID Horizontal Smooth Tube: Comparison with the Low GWP Substitute R32. *International Journal of Heat and Mass Transfer* 2018;125:702–709.
- [20] Longo G.A., Mancin S., Righetti G., Zilio C., Saturated Vapour Condensation of R134a inside a 4 mm ID Horizontal Smooth Tube: Comparison with the Low GWP Substitutes R152a, R1234yf and R1234ze(E). *International Journal of Heat and Mass Transfer* 2019;133:461–473.
- [21] Ghim G., Lee J., Condensation Heat Transfer of Low GWP ORC Working Fluids in a Horizontal Smooth Tube. *International Journal of Heat and Mass Transfer* 2017;104:718–728.
- [22] Patel T., Parekh A.D., Tailor P.R., Experimental Analysis of Condensation Heat Transfer and Frictional Pressure Drop in a Horizontal Circular Mini Channel. *Heat and Mass Transfer/Waerme- und Stoffuebertragung* 2020;56:1579–1600.



- [23] Zhuang X.R., Gong M.Q., Zou X., Chen G.F., Wu J.F., Experimental Investigation on Flow Condensation Heat Transfer and Pressure Drop of R170 in a Horizontal Tube. *International Journal of Refrigeration* 2016;66:105–120.
- [24] Song Q., Chen G., Xue H., Zhao Y., Gong M., R14 Flow Condensation Heat Transfer Performance: Measurements and Modeling Based on Two-Phase Flow Patterns. *International Journal of Heat and Mass Transfer* 2019;136:298–311.
- [25] Zhuang X.R., Chen G.F., Zou X., Song Q.L., Gong M.Q., Étude Expérimentale Sur La Condensation De L'Écoulement De Méthane Dans Un Tube Horizontal Lisse. *International Journal of Refrigeration* 2017;78:193–214.
- [26] Milkie J.A., Condensation of Hydrocarbons and Zeotropic Hydrocarbon/Refrigerant Mixtures in Horizontal Tubes. 2014;
- [27] Keniar K., Garimella S., Experimental Investigation of Refrigerant Condensation in Circular and Square Micro- and Mini- Channels. *International Journal of Heat and Mass Transfer* 2021;176:121383.
- [28] Moreira T.A., Ayub Z.H., Ribatski G., Convective Condensation of R600a, R290, R1270 and Their Zeotropic Binary Mixtures in Horizontal Tubes. *International Journal of Refrigeration* 2021;130:27–43.
- [29] Huang X., Ding G., Hu H., Zhu Y., Peng H., Gao Y., Deng B., Influence of Oil on Flow Condensation Heat Transfer of R410A inside 4.18 Mm and 1.6 Mm Inner Diameter Horizontal Smooth Tubes. *International Journal of Refrigeration* 2010;33:158–169.
- [30] Illán-Gómez F., López-Belchí A., García-Cascales J.R., Vera-García F., Experimental Two-Phase Heat Transfer Coefficient and Frictional Pressure Drop inside Mini-Channels during Condensation with R1234yf and R134a. *International Journal of Refrigeration* 2015;51:12–23.
- [31] Del Col D., Azzolin M., Bortolin S., Berto A., Experimental Results and Design Procedures for Minichannel Condensers and Evaporators Using Propylene. *International Journal of Refrigeration* 2017;83:23–38.
- [32] Azzolin M., Bortolin S., Del Col D., Convective Condensation at Low Mass Flux: Effect of Turbulence and Tube Orientation on the Heat Transfer. *International Journal of Heat and Mass Transfer* 2019;144:118646.
- [33] Berto A., Lavieille P., Azzolin M., Bortolin S., Miscevic M., Del Col D., Liquid Film Thickness and Heat Transfer Measurements during Downflow Condensation inside a Small Diameter Tube. *International Journal of Multiphase Flow* 2021;140:103649.
- [34] Niksa-Rynkiewicz T., Witkowska A., Gluch J., Adamowicz M., Monitoring the Gas Turbine Start-up Phase on the Platform Using a Hierarchical Model Based on Multi-Layer Perceptron Networks. *Polish Maritime Research* 2022;
- [35] Niksa-Rynkiewicz T., Szewczuk-Krypa N., Witkowska A., Cpałka K., Zalański M., Cader A., Monitoring Regenerative Heat Exchanger in Steam Power Plant by Making Use of the Recurrent Neural Network. *Journal of Artificial Intelligence and Soft Computing Research* 2021;
- [36] Goodfellow I., Bengio Y., Courville A., *Deep Learning*. Cambridge: MIT Press, 2016;